Phason dynamics in nonlinear photonic quasicrystals

BARAK FREEDMAN[1], RON LIFSHITZ[2], JASON W. FLEISCHER[3] AND MORDECHAI SEGEV[1]*

[1]Physics Department and Solid State Institute, Technion - Israel Institute of Technology, Haifa 32000, Israel
[2]School of Physics & Astronomy, Raymond and Beverly Sackler Faculty of Exact Sciences, Tel Aviv University, Tel Aviv 69978, Israel
[3]Department of Electrical Engineering, Princeton University, Princeton, New Jersey 08544, USA
*e-mail: msegev@tx.technion.ac.il

Published online: 12 August 2007; doi:10.1038/nmat1981

We study the dynamics of phasons in a nonlinear photonic quasicrystal. The photonic quasicrystal is formed by optical induction, and its dynamics is initiated by allowing the light waves inducing the quasicrystal to nonlinearly interact with one another. We show quantitatively that, when phason strain is introduced in a controlled manner, it relaxes through the nonlinear interactions within the photonic quasicrystal. We establish experimentally that the relaxation rate of phason strain in the quasicrystal is substantially lower than the relaxation rate of phonon strain, as predicted for atomic quasicrystals. Finally, we monitor and identify individual 'atomic-scale' phason flips occurring in the photonic quasicrystal as its phason strain relaxes, as well as noise-induced phason fluctuations.

Quasicrystals are a phase of solid matter, with long-range positional order and no periodicity[1,2]. This geometry means that quasicrystals may have symmetries, and show other physical characteristics, that cannot exist in periodic crystals[3]. Phasons, for example, are collective excitations that are unique to quasiperiodic crystals. They owe their existence to the fact that it is possible to carry out non-trivial global rearrangements of the atomic positions in a quasicrystal without affecting its free energy, thus leaving it in its ground state. In contrast, in a periodic crystal, the only non-trivial transformations that leave it in its ground state are rigid-body translations by vectors $\mathbf{u}$, taken from within the unit cell (and rotations that are irrelevant in this context). When the translation is allowed to vary slowly as a function of position $\mathbf{r}$, defining a strain field $\mathbf{u}(\mathbf{r})$, the free energy slightly increases. Such a strain field is described in terms of phonons—low-energy collective excitations of the crystal—that arise as a direct consequence of Goldstone's theorem[4]. Similarly, the global rearrangements of the atomic positions in a quasicrystal, that do not change its free energy, may be parameterized by another vector, $\mathbf{w}$. When this vector is allowed to vary slowly in space, we obtain a so-called phason-strain field $\mathbf{w}(\mathbf{r})$, described in terms of different low-energy collective excitations of the crystal, called phasons.

The existence of phasons as fundamental degrees of freedom, affecting the physical behaviour of quasicrystals, has been clearly established over the years. Their role in a generalized elasticity or hydrodynamic theory of quasicrystals[2] was developed in a series of papers[5–12] immediately following the discovery of quasicrystals[1]. Phasons have been observed in numerous experiments, whether directly or indirectly, throughout the past two decades[13–18], yet they are still a source of interesting analytical puzzles[19] and ongoing debate[20]. In this article, we shed new light on the understanding of phasons by studying their dynamics in a new form of quasicrystalline medium—an optically induced nonlinear photonic quasicrystal—which we have recently demonstrated[21]. This optically induced photonic quasicrystal serves as an excellent means for studying linear and nonlinear wave phenomena in quasicrystals, ranging from wave tunnelling and solitons to dislocation dynamics[21]. As such, it joins a host of soft-matter systems[22–27] and artificially constructed metamaterials[28–33] in which the relatively large 'inter-atomic' separation facilitates direct observations of the internal dynamics of a quasicrystal at its own 'atomic' scale. The typical distance between crystal sites in our photonic quasicrystal is 15−30 μm.

Here, we concentrate on two types of experiment, demonstrating that the dynamics governing the nonlinear photonic quasicrystal relax any phonon-strain fields or phason-strain fields that are initially imposed on it, that is, that a perturbed quasicrystal tends towards a perfectly ordered quasiperiodic structure without any strain. Furthermore, we clearly establish that the relaxation rate of phason strain in the photonic quasicrystal is substantially slower than the relaxation rate of phonon strain, as expected from theory[5–9,11], even though this is not a solid-state quasicrystal in which phason strain relaxes through the actual diffusion of matter through the crystal. Finally, we monitor the individual phason flips occurring in our photonic quasicrystal as the phason strain relaxes, and visualize elementary noise-induced phason fluctuations. These noise-induced phason fluctuations are analogous to the thermally induced phason fluctuations seen in atomic quasicrystals, as recently observed by Edagawa *et al.*[16,17].

We produce two-dimensional photonic quasicrystals by using the optical induction technique[34,35] that has recently become a useful tool in studying solitons in two-dimensional nonlinear optical lattices[36–39] and Anderson localization phenomena[40]. This technique relies on the interference of several monochromatic light beams, whereby the resulting intensity pattern is translated into a (periodic or quasiperiodic) change in the refractive index of a photosensitive nonlinear material, in this case a photorefractive SBN:60 ($Sr_{0.6}Ba_{0.4}Nb_2O_6$) crystal. This spatially varying index of refraction affects only light that is polarized in a certain direction (extraordinary polarization in our SBN:60 sample). Light that is polarized in the orthogonal direction (ordinary polarization in SBN:60) propagates through the medium as if its

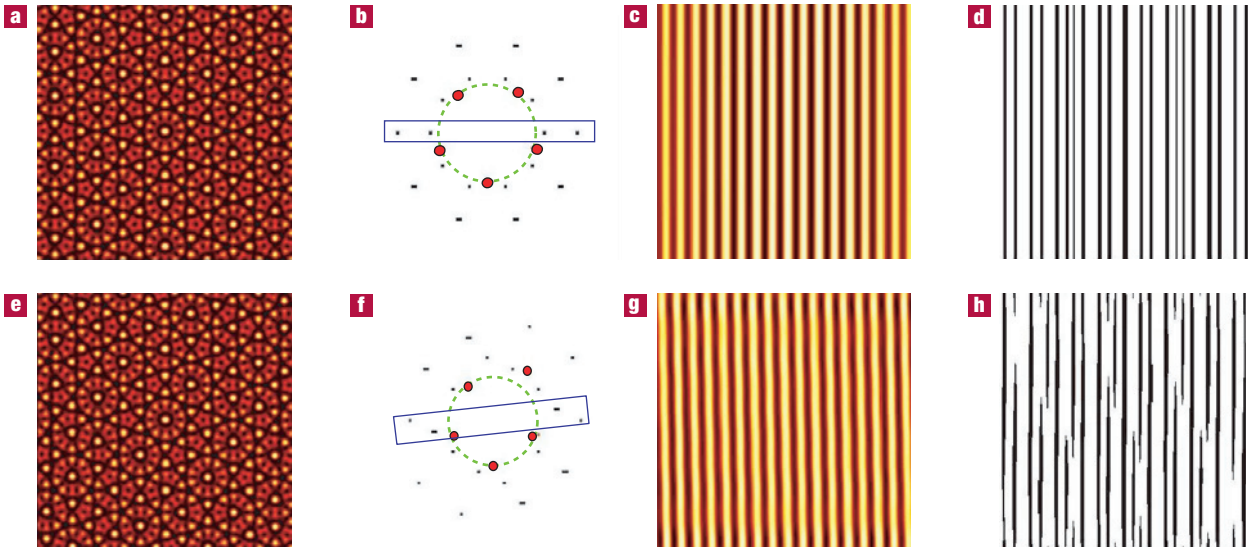

Figure 1 Numerically constructed photonic quasicrystals, with and without a static linear phason-strain field. a, Real-space image of a perfect decagonal photonic quasicrystal, as defined by equation (2) and as expected at the output face of the SBN:60 sample for non-interacting ordinarily polarized lattice-forming beams. **b**, The black spots comprise the Fourier transform of the real-space image. Superposed are five red spots representing the five optical waves inducing the structure. The black spots are the Bragg peaks of the quasicrystal itself. **c**, A single intensity wave, obtained by filtering only the two inner spots within the blue rectangle shown in **b**. **d**, Image obtained by filtering the four Bragg peaks contained within the blue rectangle. This corresponds to two intensity waves whose wavevectors are related by a factor of the golden ratio. Consequently, the distances between the stripes follow the Fibonacci sequence. **e–h**, The same as **a–d** respectively after adding a static linear phason-strain field as described by equation (3). One of the lattice-forming beams is shifted so that it lies outside the original circle. Phason strain is visible as 'jags' in **h**, as explained in the text.

refractive index were homogeneous. To study phason dynamics, we 'turn on' the interaction between the lattice-forming beams by using extraordinary polarization, thus allowing the beams to interact through the spatial variations in the refractive index that the beams themselves induce. The structure we obtain can be thought of as a quasicrystal of solitons, interacting with one another. In the low-intensity limit of the photorefractive screening nonlinearity[41], this interaction in our photonic quasicrystal gives rise to complex nonlinear dynamics[21,40], which is governed by the so-called nonlinear Schrödinger equation[42],

$$i\frac{\partial\psi}{\partial z}+\frac{1}{2k}\left(\frac{\partial^2\psi}{\partial x^2}+\frac{\partial^2\psi}{\partial y^2}\right)+\Delta n_0|\psi|^2\psi=0, \qquad (1)$$

where ψ is the extraordinarily polarized light field inducing the quasicrystal and interacting with the nonlinear refractive index change it induces, $k=k_0n_e$ is the optical wavenumber in the medium, k_0 is the vacuum wavenumber, n_e is the relevant refractive index and $\Delta n_0=k_0n_e^3r_{33}V/(2L)$, with V being the voltage applied to the crystal between electrodes separated by a distance L, and r_{33} the relevant electro-optic coefficient. Here, the intensity of the light beams inducing the lattice $|\psi|^2$ is measured compared with the intensity of a uniform background illumination, which is copropagating with the lattice-forming beams[41]. In this setting, the two-dimensional quasicrystalline ordering is in the xy plane, whereas the evolution of the system is in the propagation coordinate z; hence, the time variable t known from the quantum-mechanical version of the nonlinear Schrödinger equation is replaced in equation (1) by the propagation distance z. Thus, our measurements are limited by the propagation length through our SBN:60 samples, which is equivalent to observing the temporal dynamics of the quasicrystal after a finite evolution time[40]. Nevertheless, we have the ability to increase the strength Δn_0 of the nonlinear interaction by varying the applied voltage V, effectively viewing later 'times' (optical path lengths $(n_0+\Delta n_0)d$) in the dynamics, for a fixed propagation distance d within the sample. In the discussion that follows, we refer to the SBN:60 crystal as the 'sample', and to the dynamical field-intensity pattern $|\psi(x,y)|^2$ as the 'photonic structure', or when appropriate as the 'photonic quasicrystal'.

As in ref. 21, we generate a decagonal photonic quasicrystal by overlapping five coherent monochromatic laser beams with wavevectors $\mathbf{k}_m=(\cos(2\pi m/5),\sin(2\pi m/5))$, $m=0,\ldots,4$. The induced field-intensity pattern is given by

$$|\psi(\mathbf{r})|^2=\left|\sum_{m=0}^{4}e^{i\,\mathbf{k}_m\cdot\mathbf{r}}\right|^2, \qquad (2)$$

consisting of a d.c. $\mathbf{k}=0$ component, and exactly 20 harmonic components with wavevectors of the form $\mathbf{k}_i-\mathbf{k}_j$, where $i,j=0,\ldots,4$. A numerical image of the quasicrystal generated in this manner is shown in Fig. 1a and its 2D Fourier transform in Fig. 1b, with red dots added to mark the wavevectors of the lattice-forming beams. We have shown in ref. 21 that for extraordinary polarization the nonlinear interactions between the lattice-forming beams generate additional harmonics beyond the initial 20, thus producing a fully fledged quasicrystal. Furthermore, we have established in ref. 21 that the crystal shown in Fig. 1a remains stable throughout the propagation length of the SBN:60 sample when the nonlinear interactions are 'turned on'. Thus, when we introduce strain or defects into the quasicrystal, it evolves, under the dynamics imposed by the nonlinear Schrödinger equation (1), to recover a perfect quasicrystal ground state, as the one shown in Fig. 1a. For comparison with the phason-strained quasicrystal, which we discuss next, we show in Fig. 1c one of the field-intensity waves, making up the perfect quasicrystal, after a pair of Bragg peaks (making up a single intensity wave) have been filtered

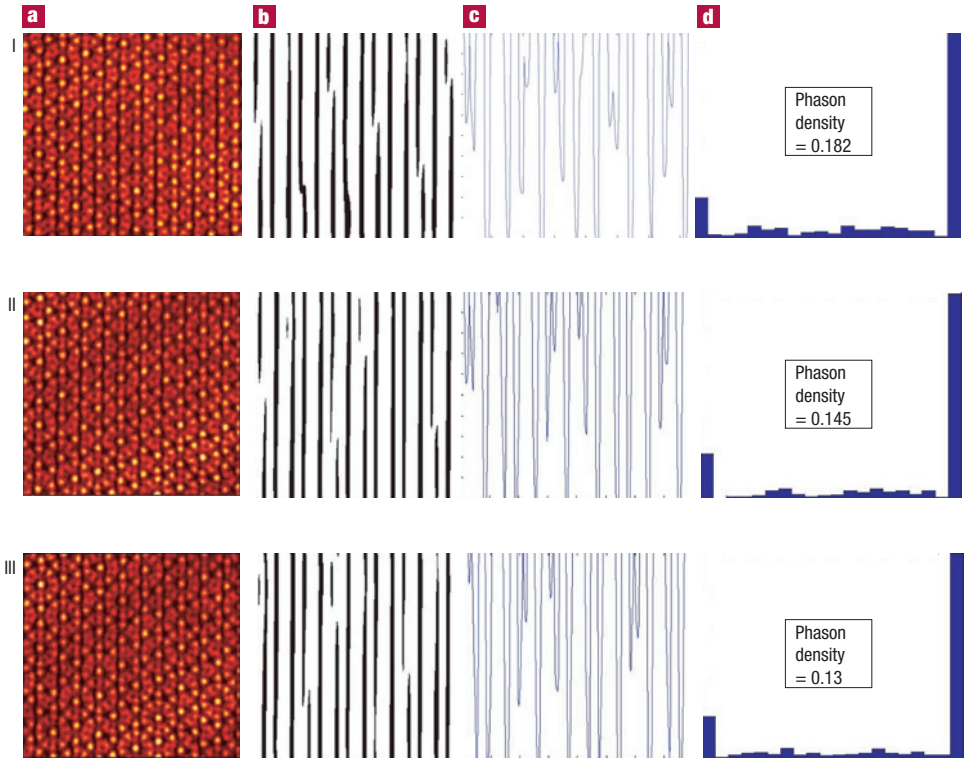

Figure 2 Experimental observation of the relaxation of a linear phason-strain field in a photonic quasicrystal. I. A non-interacting photonic quasicrystal where the induced strain field remains unaffected all the way to the output face of the sample. II. A photonic quasicrystal with nonlinear interactions turned on by changing the polarization of the lattice-forming beams to extraordinary. The phason-strain field is partially relaxed as seen by a smaller density of jags. III. A photonic quasicrystal with stronger nonlinear interactions. The strain field is further relaxed. In each row **a** shows the real-space image of the quasicrystal at the output face of the sample, **b** shows the stripe pattern obtained by filtering two intensity waves, approximately related by a factor of the golden ratio τ, **c** shows an integration of the data in **b** along the direction of the stripes and **d** shows a histogram of stripe lengths in the patterns in **b**, with the fraction of stripes of length other than zero or unity giving a quantitative indication of the remaining degree of phason strain at the output face.

out of the Fourier transform in Fig. 1b and transformed back to real space (as in ref. 43). The same is done in Fig. 1d, with some contrast enhancement, but for two pairs of Bragg peaks at τ-related wavevectors, where $\tau = (1+\sqrt{5})/2$ is the golden ratio. The distances between the stripes in Fig. 1d follow the well-known Fibonacci sequence of long (L) and short (S) distances, LLSLLSLSLLSLS....

It is now essential to recall[7,10] that one of the signatures of a quenched linear phason-strain field in a quasicrystal—a phason-strain field $\mathbf{w}(\mathbf{r})$ that varies linearly with $\mathbf{r}$—is the appearance of anisotropic shifts in the positions of Bragg peaks in the diffraction pattern of the quasicrystal, with weak-intensity peaks showing greater distortion than brighter peaks. In our first set of experiments, we mimic such a quenched phason-strain field by introducing a slight shift $\Delta\mathbf{k}$ in the position of one of the lattice-forming beams $\mathbf{k}_0$. This leads to a field-intensity pattern given by

$$|\psi(\mathbf{r})|^2 = \left| e^{i(\mathbf{k}_0+\Delta\mathbf{k})\cdot\mathbf{r}} + \sum_{m=1}^{4} e^{i\,\mathbf{k}_m\cdot\mathbf{r}} \right|^2 . \qquad (3)$$

We produce this effective shift in the position of one of the five writing beams by altering its input angle into the SBN:60 sample. In Fig. 1e–h we show a numerical image of such a quasicrystal with an exaggerated $\Delta\mathbf{k}$, along with its Fourier transform and filtered intensity waves. Phason strain is evident in Fig. 1h by the existence of points where the distances between the Fibonacci stripes change from LS to SL and *vice versa*, reflecting a position-dependent change in the relative phase of the two τ-related waves. These 'jags' in the pattern of stripes indicate the existence of local 'atomic' rearrangements in the full quasicrystal—local phason flips—with respect to the perfect quasicrystal. The greater the phason strain, relative to the perfect quasicrystal, the larger the density of these jags. Note that the pattern of lines of a single intensity wave, shown in Fig. 1g, is perfectly straight, indicating that there is no phonon strain present in the quasicrystal, even though it has phason strain.

Figure 2 shows an experimental phason-strained photonic quasicrystal, where the strain is formed as described above. Each row of plates corresponds to a different experimental situation, ranging from no nonlinear interaction to strong interaction dynamics. Consider first columns a and b of Fig. 2, showing the real-space images of the photonic quasicrystals, and the patterns of stripes obtained after filtering pairs of intensity waves related approximately by a factor of the golden ratio τ (as shown above for the numerical images in Fig. 1). In the first row, phason strain is introduced using non-interacting ordinarily polarized lattice-forming beams. The strain persists throughout the propagation distance within the sample and is observed at the output face, as is evident from the relatively high density of jags. The second row depicts the output face of the sample, after changing the polarization of the same input beams, thus turning on the dynamics. We can qualitatively see that the phason-strain field has partially relaxed by noting a reduction in the density of jags. In the third row, a stronger nonlinear interaction is applied, rendering

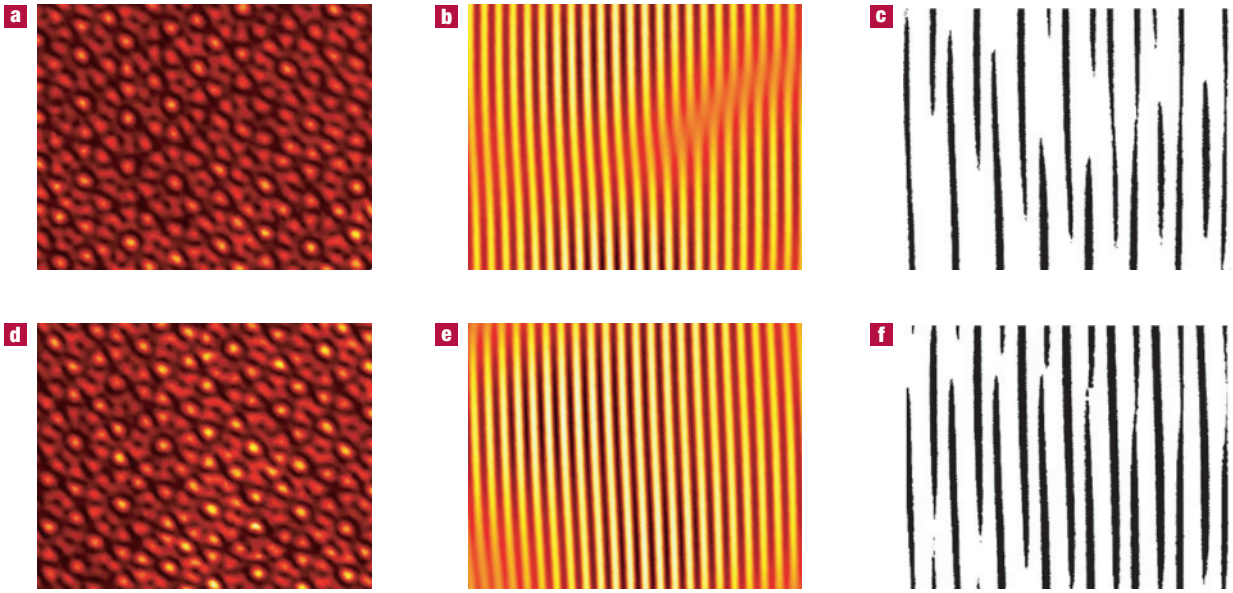

Figure 3 Experimental observation of phonon-strain and phason-strain relaxation following the injection of a dislocation into a photonic quasicrystal. **a**, Non-interacting photonic quasicrystal with an embedded (1, 0, 0, 0) dislocation. **b**, The dislocation is made visible by filtering one intensity wave in the Fourier spectrum. Notice that the lines are distorted, indicating the existence of phonon strain. **c**, Phason strain is made visible by jags that appear after filtering two τ-related intensity waves from the Fourier spectrum. **d**, The same quasicrystal with the interaction turned on, showing that the dislocation has been removed. **e**, Filtering one intensity wave shows straight lines, indicating the healing of the dislocation as well as the relaxation of phonon strain. **f**, Filtering of two τ-related intensity waves shows that phason strain still remains in the structure, establishing that its relaxation rate is lower than that of phonon strain.

faster relaxation and fewer jags as the beams propagate down the sample. The output face in this case shows further relaxation of the strain field, indicated by even fewer jags in the striped pattern.

To obtain statistically meaningful quantitative data that can clearly establish the relaxation of phason strain due to nonlinear interactions, as the waves propagate through the sample, we repeat each measurement 30 times. To calculate the degree of phason strain efficiently, we integrate each contrast-enhanced pattern of stripes along the stripe direction, as shown in column c of Fig. 2, and calculate a histogram (representing an averaging over 30 experiments) of stripe lengths, shown in column d. The histogram of a perfect quasicrystal, lacking any strain, would show stripes only of zero or unit length. The degree of phason strain is given by the relative number of partial stripes in the pattern, filling the bins between zero and unity. Although this is not an absolute measure of phason strain, it enables a quantitative comparison between the different experimental situations (replacing the perpendicular-space analysis of refs 16,17). Averaging over 30 realizations of each situation, we find that the mean values have only 2.5% standard deviation, thus indicating the significance of the result. As manifested by the histograms in column d, we clearly observe the relaxation of phason strain in our dynamical photonic quasicrystal due to the nonlinear interactions, which eventually take it to its ground state.

In our second set of experiments, we induce a more natural strain field, containing both phason and phonon components, by injecting a dislocation into the photonic quasicrystal[21,43]. This is achieved by converting one of the writing beams into a vortex beam[44], and obtaining a field-intensity pattern given by

$$|\psi(\mathbf{r})|^2 = \left| e^{i(\mathbf{k}_0\cdot\mathbf{r}+\varphi(\mathbf{r}))} + \sum_{m=1}^{4} e^{i\,\mathbf{k}_m\cdot\mathbf{r}} \right|^2, \qquad (4)$$

where $\varphi(\mathbf{r})$ is the usual azimuthal polar coordinate. In ref. 21 we have shown that such a dislocation, with Burgers vector $(1,0,0,0)$, eventually disappears when nonlinear interactions are turned on. Here, we examine what remains of the quasicrystal after the healing of the dislocation.

Recall that in an atomic quasicrystal the relaxation of phonon strain via the propagation of sound waves is expected to occur relatively quickly. On the other hand, the relaxation of phason strain is a process that requires atomic rearrangements. It is therefore expected to be a much slower process, on the basis of the diffusive motion of atoms relative to one another. For soft-matter quasicrystals, or the photonic quasicrystals studied here, we might expect the wave-dynamics situation to be different. Here, owing to the softness, different density waves could presumably move through one another to relieve phason strain without the need for diffusive rearrangements of atomic positions. Such a process is impossible in the case of 'hard-core' atoms that cannot penetrate one another. Nevertheless, coarse-grained density-wave and hydrodynamic theories of quasicrystals also predict that the process of phason-strain relaxation should be diffusive and therefore slower than that of phonon-strain relaxation. It is therefore important to determine experimentally whether phason relaxation in quasicrystals is generically slower than phonon relaxation, regardless of the actual physical realization of the quasicrystal.

This question is resolved in the set of experiments depicted in Fig. 3. Figure 3a–c shows an experimental image of a decagonal quasicrystal with the $(1,0,0,0)$ dislocation given by equation (4), produced by non-interacting ordinarily polarized lattice-forming beams. Figure 3b reveals the existence of the dislocation at the output face of the sample by filtering a single field-intensity wave, clearly showing the discontinuation of one of the stripes at the position of the dislocation. Phonon strain is evident from the

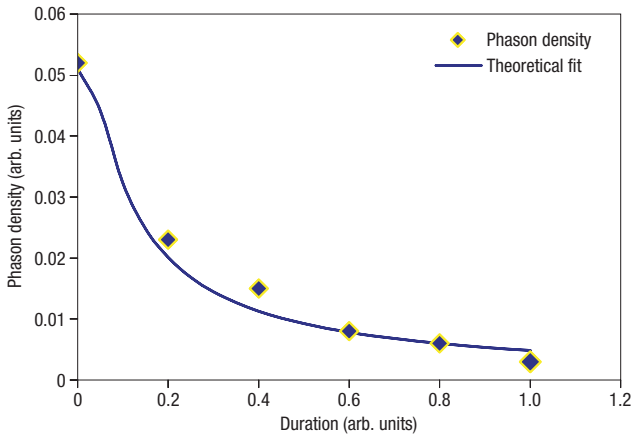

Figure 4 Effect of nonlinear interactions on phason density—measurements showing the exponential decay of the phason density. The duration of the interaction was controlled by changing the voltage applied to the photorefractive crystal. A higher voltage corresponds to a stronger interaction, which is effectively a longer interaction time. The results show an exponential decay of phason density (red, experiment; blue, best fit to the solution of the diffusion equation), which is consistent with diffusive behaviour.

distortion of the lines in this figure. Phason strain is evident from the existence of jags in the striped pattern in Fig. 3c, obtained, as in the first set of experiments, by filtering a pair of τ-related intensity waves. Figure 3d–f shows the same quasicrystal after interaction has been turned on by changing the polarization of the lattice-forming beams. Figure 3e shows that the dislocation has been removed, and that the duration of the interaction was sufficiently long to remove all phonon strain, yielding perfectly straight lines (as in the theoretical images in Fig. 1). On the other hand, Fig. 3f shows that some phason strain is still present, although to a lesser degree than in the non-interacting quasicrystal in Fig. 3c. This clearly establishes that phason strain relaxes at a significantly lower rate than phonon strain, even in our photonic quasicrystal, and therefore that this is very likely a generic property of all physical quasicrystals.

The results presented in Fig. 3 establish that phasons relax more slowly than phonons, but do not determine that the phason relaxation is indeed diffusive. Ideally, we would do this by propagating the dynamics for progressively longer distances (times), imaging the output and analysing the wave-number dependence of phason-strain relaxation. However, our crystal has a fixed length, and we cannot image the structure (or the optical intensity) within it, because the refractive index in the medium is homogeneous, as it contains the quasicrystal structure. Instead, we effectively simulate longer propagation dynamics by observing the output face of the sample ($z = d$) as we increase the applied voltage V, thus increasing the effective optical path length[36] $[n_0 + \Delta n_0(V)]d$. This effectively increases the duration of the dynamics (the evolution distance z) and yields structures at the output face that come closer and closer to the perfect ground state as the interaction is increased. This behaviour is demonstrated in Fig. 4, which shows the experimental measurement of the phason density ρ_{phason} that remains at the output face of the sample as a function of the strength of the nonlinear interaction (applied voltage, ref. 36), while keeping all other parameters unchanged. The blue line in Fig. 4 shows the best fit of the experimental results to the solution of the diffusion equation. These results clearly show an exponentially decreasing phason density with effective propagation length. That is, we establish quantitatively that as the structure approaches the perfect ground state the decay in phason density is exponential, consistent with the hydrodynamic theory of quasicrystals[6].

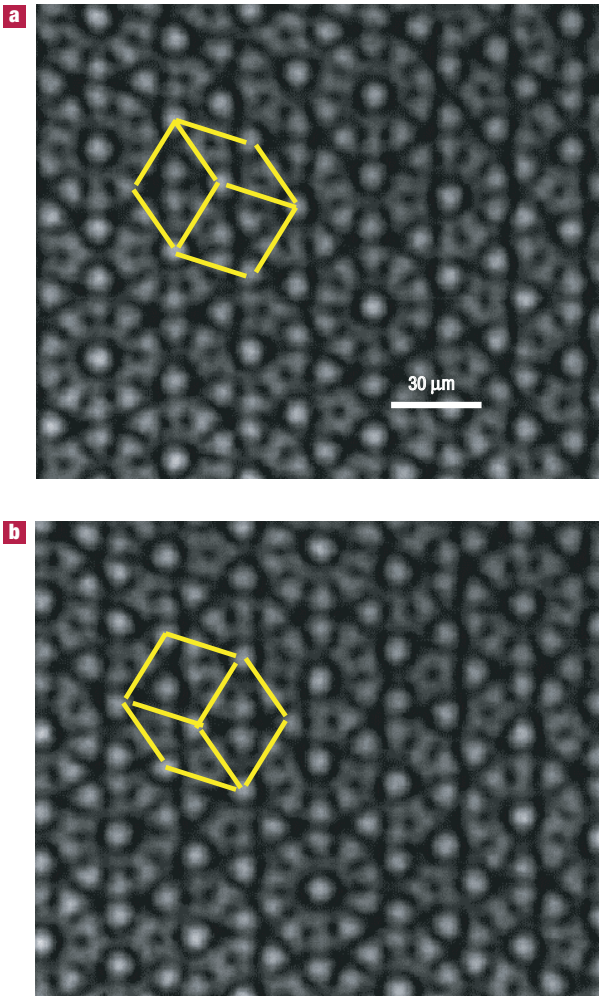

Figure 5 Direct observation of phason flips that occur as a phason-strained photonic quasicrystal relaxes to its ground state. Two frames taken from Supplementary Information, Movie M1, in which the nonlinear interaction is gradually increased to simulate the temporal evolution towards the perfectly ordered ground state. The two images contain many unchanged spots, or fixed atomic positions, as well as shifted spots indicating atomic rearrangements. One typical example is marked by a set of three tiles that change their mutual orientation as a single spot at the centre shifts its position. Note that the internal decorations of the two types of rhombic tile also adjust according to the reorientation of the tiles. Similar phason flips can be observed throughout the quasicrystal by comparing the two frames.

Finally, we show the actual local 'atomic' rearrangements, or phason flips, that occur in our photonic quasicrystal by making direct comparisons of real-space images of the quasicrystal. To do so, we produce a movie of the intensity field at the output face of the sample. We use a strained quasicrystal, gradually increasing the strength of the nonlinear interaction, again effectively simulating the temporal dynamics of the system (see Supplementary Information, Movie M1). Figure 5 shows two frames from this movie, where a number of phason flips can be identified. One such flip is marked with a set of tiles that change their configuration during the corresponding phason flip. We emphasize that the field-intensity spots, visualized in

these frames, are the smallest 'atomic' features in our photonic quasicrystals. Thus, our photonic quasicrystal—owing to its micrometre structure—lends itself more naturally to the direct observation of 'atomic-scale' dynamics in a quasicrystal.

As the last experiment in this article, we demonstrate noise-driven phason flips in our photonic quasicrystal. Such flips occur when we intentionally stop stabilizing the phase noise in the optical system that induces the quasicrystal. If we do not control the stability of our lasers, the induced pattern continuously jiggles around. Because most of the experimental noise in our system comes from fluctuations in the relative phases of the writing beams, the jiggling pattern is dominated by phason fluctuations. These phason fluctuations resemble thermal phason fluctuations in finite-temperature solid-state quasicrystals, although in our case they fluctuate in time while maintaining spatial uniformity throughout the quasicrystal (see Supplementary Information, Movie M2).

The dynamics of our photonic quasicrystals, as observed in our set of experiments, belongs to a large class of relaxational dynamical systems, in which interactions drive the field in question to a ground state of some effective free energy. Unlike the dissipative case, which includes collisional atomic systems, the wave system of our photonic quasicrystals obeys the dissipationless nonlinear Schrödinger equation (1). As such, the observed phason behaviour is representative of a more general hamiltonian dynamics commonly found in non-equilibrium pattern-forming systems[45]. The beauty of our results is in highlighting the universal features associated with phasons in systems with quasiperiodic ordering, irrespective of the specific details of a particular realization. Thus, even though our studies here were carried on photonic quasicrystals, they have general and broad implications for a wide range of quasiperiodically ordered matter. We therefore expect our system to continue providing valuable insight into the physics of quasicrystals in the coming years.

Received 31 December 2006; accepted 10 July 2007; published 12 August 2007.

References

1. Shechtman, D., Blech, I., Gratias, D. & Cahn, J. W. Metallic phase with long-range orientational order and no translational symmetry. *Phys. Rev. Lett.* **53**, 1951–1953 (1984).
2. Levine, D. & Steinhardt, P. J. Quasicrystals: A new class of ordered structures. *Phys. Rev. Lett.* **53**, 2477–2480 (1984).
3. Lifshitz, R. What is a crystal? *Z. Kristallogr.* **222**, 313–317 (2007).
4. Sethna, J. P. *Entropy, Order Parameters, and Complexity* Ch. 9 (Clarendon, Oxford, 2006).
5. Levine, D., Lubensky, T. C., Ostlund, S., Ramaswamy, S. & Steinhardt, P. J. Elasticity and dislocations in pentagonal and icosahedral quasicrystals. *Phys. Rev. Lett.* **54**, 1520–1523 (1985).
6. Lubensky, T. C., Ramaswamy, S. & Toner, J. Hydrodynamics of icosahedral quasicrystals. *Phys. Rev. B* **32**, 7444–7452 (1985).
7. Socolar, J. E. S., Lubensky, T. C. & Steinhardt, P. J. Phonons, phasons, and dislocations in quasicrystals. *Phys. Rev. B* **34**, 3345–3360 (1986).
8. Lubensky, T. C., Socolar, J. E. S., Steinhardt, P. J., Bancel, P. A. & Heiney, P. A. Distortion and peak broadening in quasicrystal diffraction patterns. *Phys. Rev. Lett.* **57**, 1440–1443 (1986).
9. Socolar, J. E. S. & Wright, D. C. Explanation of peak shapes observed in diffraction from icosahedral quasicrystals. *Phys. Rev. Lett.* **59**, 221–224 (1987).
10. Jarić, M. V. & Nelson, D. R. Diffuse scattering from quasicrystals. *Phys. Rev. B* **37**, 4458–4472 (1988).
11. Bancel, P. A. Comment on a paper by Linus Pauling. *Proc. Natl Acad. Sci.* **86**, 8600–8601 (1989).
12. Bancel, P. A. Dynamical phasons in a perfect quasicrystal. *Phys. Rev. Lett.* **63**, 2741–2744 (1989). *ibid* **64**, 496 (1990).
13. Jiang, J. C., Fung, K. K. & Kuo, K. H. Discommensurate microstructures in phason-strained octagonal quasicrystal phases of Mo–Cr–Ni. *Phys. Rev. Lett.* **68**, 616–619 (1992).
14. Li, H. L., Zhang, Z. & Kuo, K. H. Experimental Ammann-line analysis of phasons in the Al–Cu–Co–Si decagonal quasicrystal. *Phys. Rev. B* **50**, 3645–3647 (1994).
15. de Boissieu, M. *et al.* Diffuse scattering and phason elasticity in the AlPdMn icosahedral phase. *Phys. Rev. Lett.* **75**, 89–92 (1995).
16. Edagawa, K., Suzuki, K. & Takeuchi, S. High resolution transmission electron microscopy observation of thermally fluctuating phasons in decagonal Al–Cu–Co. *Phys. Rev. Lett.* **85**, 1674–1677 (2000).
17. Edagawa, K., Suzuki, K. & Takeuchi, S. HRTEM observation of phason flips in Al–Cu–Co decagonal quasicrystal. *J. Alloys Compounds* **342**, 271–277 (2002).
18. Francoual, S. *et al.* Dynamics of phason fluctuations in the *i*-AlPdMn quasicrystal. *Phys. Rev. Lett.* **91**, 225501 (2003).
19. Janssen, T., Radulescu, O. & Rubtsov, A. N. Phasons, sliding modes and friction. *Eur. Phys. J. B* **29**, 85–95 (2002).
20. Henley, C. L., de Boissieu, M. & Steurer, W. Discussion on clusters, phasons and quasicrystal stabilization. *Phil. Mag.* **86**, 1131–1151 (2006).
21. Freedman, B. *et al.* Wave and defect dynamics in nonlinear photonic quasicrystals. *Nature* **440**, 1166–1169 (2006).
22. Edwards, W. S. & Fauve, S. Parametrically excited quasicrystalline surface waves. *Phys. Rev. E* **47**, R788–R791 (1993).
23. Edwards, W. S. & Fauve, S. Patterns and quasi-patterns in the Faraday experiment. *J. Fluid Mech.* **278**, 123–148 (1994).
24. Lifshitz, R. & Petrich, D. M. Theoretical model for Faraday waves with multiple-frequency forcing. *Phys. Rev. Lett.* **79**, 1261–1264 (1997).
25. Zeng, X. *et al.* Supramolecular dendritic liquid quasicrystals. *Nature* **428**, 157–160 (2004).
26. Hayashida, K., Dotera, T., Takano, A. & Matsushita, Y. Polymeric quasicrystal: Mesoscopic quasicrystalline tiling in ABC star polymers. *Phys. Rev. Lett.* **98**, 195502 (2007).
27. Lifshitz, R. & Diamant, H. Soft quasicrystals—Why are they stable? *Phil. Mag.* **87**, 3021–3030 (2007).
28. Jin, C. *et al.* Band gap and wave guiding effect in a quasiperiodic photonic crystal. *Appl. Phys. Lett.* **75**, 1848–1850 (1999).
29. Zoorob, M. E., Charlton, M. D. B., Parker, G. J., Baumberg, J. J. & Netti, M. C. Complete photonic bandgaps in 12-fold symmetric quasicrystals. *Nature* **404**, 740–743 (2000).
30. Lifshitz, R., Arie, A. & Bahabad, A. Photonic quasicrystals for nonlinear optical frequency conversion. *Phys. Rev. Lett.* **95**, 133901 (2005).
31. Bratfalean, R. T., Peacock, A. C., Broderick, N. G. R., Gallo, K. & Lewen, R. Harmonic generation in a two-dimensional nonlinear quasicrystal. *Opt. Lett.* **30**, 424–426 (2005).
32. Man, W., Megens, M., Steinhardt, P. J. & Chaikin, P. M. Experimental measurement of the photonic properties of icosahedral quasicrystals. *Nature* **436**, 993–996 (2005).
33. Roichman, Y. & Grier, D. G. Holographic assembly of quasicrystalline photonic heterostructures. *Opt. Express* **13**, 5434–5439 (2005).
34. Efremidis, N. K., Christodoulides, D. N., Fleischer, J. W. & Segev, M. Discrete solitons in photorefractive optically induced photonic lattices. *Phys. Rev. E* **66**, 046602 (2002).
35. Fleischer, J. W., Carmon, T., Segev, M., Efremidis, N. K. & Christodoulides, D. N. Observation of discrete solitons in optically induced real time waveguide arrays. *Phys. Rev. Lett.* **90**, 023902 (2003).
36. Fleischer, J. W., Segev, M., Efremidis, N. K. & Christodoulides, D. N. Observation of two-dimensional discrete solitons in optically induced nonlinear photonic lattices. *Nature* **422**, 147–150 (2003).
37. Cohen, O. *et al.* Observation of random-phase lattice solitons. *Nature* **433**, 500–503 (2005).
38. Fleischer, J. W. *et al.* Observation of vortex-ring discrete solitons in 2D photonic lattices. *Phys. Rev. Lett.* **92**, 123904 (2004).
39. Neshev, D. N., Alexander, T. J., Ostrovskaya, E. A. & Kivshar, Y. S. Observation of discrete vortex solitons in optically induced photonic lattices. *Phys. Rev. Lett.* **92**, 123903 (2004).
40. Schwartz, T., Baral, G., Fishman, S. & Segev, M. Transport and Anderson localization in disordered two-dimensional photonic lattices. *Nature* **446**, 52–55 (2007).
41. Segev, M., Valley, G. C., Crosignani, B., DiPorto, P. & Yariv, A. Steady-state spatial screening solitons in photorefractive materials with external applied field. *Phys. Rev. Lett.* **73**, 3211–3214 (1994).
42. Chiao, R. Y., Garmire, E. & Townes, C. H. Self-trapping of optical beams. *Phys. Rev. Lett.* **13**, 479–482 (1964).
43. Barak, G. & Lifshitz, R. Dislocation dynamics in a dodecagonal quasiperiodic structure. *Phil. Mag.* **86**, 1059–1064 (2006).
44. Martin, H., Eugenieva, E. D., Chen, Z. & Christodoulides, D. N. Discrete solitons and soliton-induced dislocations in partially coherent photonic lattices. *Phys. Rev. Lett.* **92**, 123902 (2004).
45. Cross, M. C. & Hohenberg, P. C. Pattern formation outside of equilibrium. *Rev. Mod. Phys.* **65**, 851–1112 (1993).

Acknowledgements

We thank P. Steinhardt for ideas about inducing artificial phason-strain fields. R.L. is grateful to M. de Boissieu, M. Cross and M. Widom for useful discussions. This work was supported by the Israel Science Foundation, the Israel–USA Binational Science Foundation, the German–Israeli DIP Project and the US National Science Foundation.
Correspondence and requests for materials should be addressed to M.S.
Supplementary Information accompanies this paper on www.nature.com/naturematerials.

Competing financial interests

The authors declare no competing financial interests.